J Membrane Biol (2013) 246:529–543
DOI 10.1007/s00232-013-9565-4

# Subcellular Localization and Kinetic Characterization of a Gill ($Na^+$, $K^+$)-ATPase from the Giant Freshwater Prawn *Macrobrachium rosenbergii*

**Juliana L. França · Marcelo R. Pinto · Malson N. Lucena · Daniela P. Garçon · Wagner C. Valenti · John C. McNamara · Francisco A. Leone**

Received: 4 December 2012 / Accepted: 31 May 2013 / Published online: 20 June 2013


**Abstract** The stimulation by $Mg^{2+}$, $Na^+$, $K^+$, $NH_4^+$, and ATP of ($Na^+$, $K^+$)-ATPase activity in a gill microsomal fraction from the freshwater prawn *Macrobrachium rosenbergii* was examined. Immunofluorescence labeling revealed that the ($Na^+$, $K^+$)-ATPase α-subunit is distributed predominantly within the intralamellar septum, while Western blotting revealed a single α-subunit isoform of about 108 kDa $M_r$. Under saturating $Mg^{2+}$, $Na^+$, and $K^+$ concentrations, the enzyme hydrolyzed ATP, obeying cooperative kinetics with $V_M = 115.0 \pm 2.3$ U mg$^{-1}$, $K_{0.5} = 0.10 \pm 0.01$ mmol L$^{-1}$. Stimulation by $Na^+$ ($V_M = 110.0 \pm 3.3$ U mg$^{-1}$, $K_{0.5} = 1.30 \pm 0.03$ mmol L$^{-1}$), $Mg^{2+}$ ($V_M = 115.0 \pm 4.6$ U mg$^{-1}$, $K_{0.5} = 0.96 \pm 0.03$ mmol L$^{-1}$), $NH_4^+$ ($V_M = 141.0 \pm 5.6$ U mg$^{-1}$, $K_{0.5} = 1.90 \pm 0.04$ mmol L$^{-1}$), and $K^+$ ($V_M = 120.0 \pm 2.4$ U mg$^{-1}$, $K_M = 2.74 \pm 0.08$ mmol L$^{-1}$) followed single saturation curves and, except for $K^+$, exhibited site–site interaction kinetics. Ouabain inhibited ATPase activity by around 73 % with $K_I = 12.4 \pm 1.3$ mol L$^{-1}$. Complementary inhibition studies suggest the presence of $F_0F_1$–, $Na^+$-, or $K^+$-ATPases, but not V($H^+$)- or $Ca^{2+}$-ATPases, in the gill microsomal preparation. $K^+$ and $NH_4^+$ synergistically stimulated enzyme activity (≈25 %), suggesting that these ions bind to different sites on the molecule. We propose a mechanism for the stimulation by both $NH_4^+$, and $K^+$ of the gill enzyme.

**Keywords** ($Na^+$, $K^+$)-ATPase · Ammonium/potassium stimulation · ATP · Gill microsome · Giant freshwater prawn · *Macrobrachium rosenbergii*

J. L. França · M. N. Lucena
Departamento de Bioquímica e Imunologia, Faculdade de Medicina de Ribeirão Preto, Universidade de São Paulo, Ribeirão Preto, SP 14040-901, Brazil

M. R. Pinto · F. A. Leone (✉)
Departamento de Química, Faculdade de Filosofia, Ciências e Letras da Universidade de São Paulo, Ribeirão Preto, Avenida Bandeirantes, 3900, Ribeirão Preto, SP 14040-901, Brazil
e-mail: fdaleone@ffclrp.usp.br

D. P. Garçon
Departamento de Biologia Molecular, Centro de Ciências Exatas e da Natureza, Universidade Federal da Paraíba, João Pessoa, PB 58059-900, Brazil

W. C. Valenti
Campus Experimental do Litoral Paulista, Universidade Estadual Paulista Júlio de Mesquita Filho, São Vicente, SP 11330-900, Brazil

J. C. McNamara
Departamento de Biologia, Faculdade de Filosofia, Ciências e Letras da Universidade de São Paulo, Ribeirão Preto, SP 14040-901, Brazil

## Introduction

The giant freshwater prawn, *Macrobrachium rosenbergii*, is endemic to the Indo-Pacific region, northern Australia, and southeastern Asia, where it typically inhabits freshwater environments and migrates to estuarine or brackish waters to spawn. The species is a hyperosmoregulator in freshwater and at low salinities and hypo-osmoregulates in higher salinities up to 25 ‰ (Wilder et al. 1998), tolerating a wide range of temperatures, 14–35 °C (New 1995). Temperature, pH and salinity all influence oxygen consumption and nitrogen excretion in *M. rosenbergii* (Chen and Kou 1996). Ammonia plays a role in crustacean osmoregulation as a counter-ion for $Na^+$ uptake to the hemolymph (Kirschner 1979; Augusto et al. 2007), and in *M. rosenbergii*, $NH_4^+$ excretion is balanced by $Na^+$ uptake, requiring either an

$Na^+/NH_4^+$ exchanger or the ($Na^+$, $K^+$)-ATPase as the carrier enzyme (Towle and Taylor 1976).

The ($Na^+$, $K^+$)-ATPase, the most prominent member of the P-type ATPases (Pedersen and Amzel 1993; Chourasia and Sastry 2012), pumps three $Na^+$ out of and two $K^+$ into cells per molecule of ATP hydrolyzed. The pump creates opposing $Na^+$ and $K^+$ concentration gradients across the plasma membrane, maintains the resting potential of neurons and other excitable cells and drives diverse secondary transport systems (Horisberger 2004). The enzyme consists of three subunits (Kaplan 2002; Garty and Karlish 2006; Geering 2008; Poulsen et al. 2010; Toyoshima et al. 2011). The 95- to 110-kDa α-subunit or catalytic subunit is formed by 10 transmembrane segments (Garty and Karlish 2006) and contains the protein kinase phosphorylation domain and the nucleotide-, cation- and cardiotonic steroid–binding sites (Kaplan 2002; Lingrel 2010). The 55- to 60-kDa β-subunit is highly glycosylated and acts as a chaperone (Poulsen et al. 2010). The 6.5- to 7.5-kDa γ-subunit, known as an FXYD protein, modulates the vertebrate ($Na^+$, $K^+$)-ATPase in a tissue-specific manner (Geering 2008). Recently, the γ-subunit was demonstrated to comprise a functional constituent of the crustacean ($Na^+$, $K^+$)-ATPase (Silva et al. 2012).

The multifunctional gills, together with the excretory organs, are mainly responsible for osmotic and ionic regulation in the Crustacea (Péqueux 1995; Freire et al. 2008). The gill epithelial cells also play a central role in hemolymph acid–base regulation via cytoplasmic carbonic anhydrase and in the excretion of nitrogenous metabolic end products (Péqueux 1995; Lucu and Towle 2003). McNamara and Lima (1997), Freire et al. (2008), Faleiros et al. (2010) and McNamara and Faria (2012) have developed a widely accepted transport model for strongly hyperosmoregulating palaemonids, like *M. rosenbergii*, in which two intimately coupled gill cell types drive salt uptake. Deep invaginations of the intralamellar septal cell membranes contain the ($Na^+$, $K^+$)-ATPase (McNamara and Torres 1999), together with $K^+$ and $Cl^-$ channels, and actively transport $Na^+$ to the surrounding hemolymph. The apical pillar cell flange membranes face the external medium and contain $Na^+$ channels, V-type $H^+$ pumps and $Cl^-/HCO_3^-$ exchangers, transferring their salt load via the pillar cell perikarya to the septal cells to which they are structurally coupled. Although ($Na^+$, $K^+$)-ATPase-specific activity increases in most euryhaline marine crustaceans acclimated to dilute media (Lucu and Towle 2003; Genovese et al. 2004; Garçon et al. 2009; Torres et al. 2007), such activity is apparently unaltered when *M. rosenbergii* is acclimated to different salinities (Wilder et al. 2000) or during its molt cycle (Jasmani et al. 2008).

In this study, we investigate the cellular localization of ($Na^+$, $K^+$)-ATPase by immunofluorescence labeling in gill lamellae of the giant freshwater prawn *M. rosenbergii* and provide an extensive kinetic characterization of ($Na^+$, $K^+$)-ATPase activity in a gill microsomal fraction, including a detailed description of the synergistic stimulation of enzyme activity by $NH_4^+$ and $K^+$.

## Materials and Methods

### Materials

All solutions were prepared using Millipore (Billerica, MA) MilliQ ultrapure, apyrogenic water. Tris, ATP ditris salt, pyruvate kinase (PK), phosphoenolpyruvate (PEP), $NAD^+$, NADH, imidazole, *N*-(2-hydroxyethyl) piperazine-*N*′-ethanesulfonic acid (HEPES), lactate dehydrogenase (LDH), ouabain, glyceraldehyde-3-phosphate dehydrogenase (GAPDH), phosphoglycerate kinase (PGK), glyceraldehyde-3-phosphate (G3P), alamethicin, imidazole, 4′,6-diamidino-2-phenylindole (DAPI), bovine serum albumin (BSA), sodium orthovanadate, gelatin-coated slides (225 bloom), 3-phosphoglyceraldehyde diethyl acetal, ethacrynic acid, oligomycin, thapsigargin and bafilomycin $A_1$ were purchased from Sigma (St. Louis, MO). Dimethyl sulfoxide and triethanolamine were from Merck (Darmstadt, Germany). The protease inhibitor cocktail (1 mmol $L^{-1}$ benzamidine, 5 μmol $L^{-1}$ antipain, 5 μmol $L^{-1}$ phenyl methane-sulfonyl-fluoride, 5 μmol $L^{-1}$ Leupeptin and 1 μmol $L^{-1}$ pepstatin A) was from Calbiochem (Darmstadt, Germany). Optimal Cutting Temperature Compound was from Sakura Tissue-Tek (Torrance, CA). Paraformaldehyde was from Electron Microscopy Sciences (Hatfield, PA). The mouse monoclonal antibody IgG α-5 raised against the α-subunit of the chicken ($Na^+$, $K^+$)-ATPase was from the Development Studies Hybridoma Bank, maintained by the University of Iowa (Iowa City, IA). Alexafluor 488, donkey anti-mouse IgG, was from Invitrogen (Carlsbad, CA), and fluoromount-G was from Electron Microscopy Sciences; all other reagents were of the highest purity commercially available.

Crystalline suspensions in 2.9 mol $L^{-1}$ ammonium sulfate solution (200 μL) of LDH and PK were centrifuged at 14,000 rpm for 15 min at 4 °C in an Eppendorf model 5810 refrigerated centrifuge. The pellet was resuspended in 500 μL of 50 mmol $L^{-1}$ HEPES buffer (pH 7.5), transferred to a YM-10 Microcon filter and washed five times at 10,000 rpm for 15 min at 4 °C in the same buffer until complete removal of ammonium ions (tested with the Nessler reagent). Finally, the pellet was resuspended to the original volume. For PGK and GAPDH, the suspension was treated as above with 50 mmol $L^{-1}$ triethanolamine buffer (pH 7.5), containing 1 mmol $L^{-1}$ dithiothreitol. Ammonium-depleted PK and LDH solutions were used within 2 days.

G3P was prepared by hydrolysis of 3-phospho-glyceraldehyde diethyl acetal, barium salt, with 150 μL HCl

($d = 1.18$ g $mL^{-1}$) in a boiling-water bath for 2 min, after removal of the barium salt with Dowex $50H^+$ resin. Final pH was adjusted to 7.0 with 50 µL triethanolamine just before use. Sodium orthovanadate solution was prepared according to Lucena et al. (2012). When necessary, enzyme solutions were concentrated on YM-10 Amicon Microcon filters.

## Prawns, Hemolymph Sampling and Gill Dissection

Broodstock of *M. rosenbergii* were produced at the Aquaculture Center, UNESP, Jaboticabal, São Paulo, Brazil. Prawns were raised in freshwater (0.65 mmol $Na^+$ $L^{-1}$, 0.04 mmol $K^+$ $L^{-1}$, 2.0 mmol $Ca^{2+}$ $L^{-1}$ and 0.21 mmol $Mg^{2+}$ $L^{-1}$) and harvested directly from the rearing tanks. They were transported to the laboratory, held in 60-L tanks containing aerated freshwater from the rearing site and processed within 2 h.

Individual hemolymph samples (200 µL) were drawn into insulin syringes using #25-8 needles from the junction of the arthrodial membrane at the base of the last pereiopod from each of three different prawns and stored at −20 °C until processing (Lucena et al. 2012).

For each gill homogenate prepared, five to eight prawns were anesthetized by chilling on crushed ice for 5 min. The prawns were killed by destroying the cerebral and thoracic ganglia. All gill pairs were excised and transferred to ice-cold homogenization buffer (20 mL $g^{-1}$ wet tissue), consisting of 20 mmol $L^{-1}$ imidazole (pH 6.8) plus 250 mmol $L^{-1}$ sucrose, 6 mmol $L^{-1}$ EDTA and a proteinase inhibitor cocktail (1 mmol $L^{-1}$ benzamidine, 5 µmol $L^{-1}$ antipain, 5 µmol $L^{-1}$ leupeptin, 1 µmol $L^{-1}$ pepstatin A and 5 µmol $L^{-1}$ phenylmethyl-sulfonyl fluoride). Finally, the gills were homogenized using a Potter homogenizer, set at 600 rpm.

## Preparation of the Gill Microsomal Fraction

The crude extract was centrifuged at 20,000×*g* for 35 min at 4 °C, the supernatant was stored over crushed ice and the pellet was resuspended in an equal volume of homogenization buffer. After further centrifugation as above, the two supernatants were gently pooled and centrifuged at 100,000×*g* for 90 min at 4 °C, and the resulting pellet was resuspended in the homogenization buffer (6 mL $g^{-1}$ wet tissue). Finally, 0.5-mL aliquots of the microsomal fraction were rapidly frozen in liquid nitrogen and stored at −20 °C. No appreciable loss of activity was seen after 2 month's storage. When required, the aliquots were thawed, placed on crushed ice and used immediately.

## Measurement of Hemolymph Cation Concentrations

Hemolymph $Na^+$, $K^+$, $Ca^{2+}$ and $Mg^{2+}$ concentrations were measured by emission spectroscopy using a Shimadzu (Kyoto, Japan) model AA-680 atomic absorption spectrophotometer employing 10-µL hemolymph aliquots diluted 1: 2,500 with Millipore MilliQ ultrapure apyrogenic water. Data are given as the mean ± SD of three different hemolymph samples.

## Measurement of ATPase Activity

ATPase activity was assayed at 25 °C using a PK/LDH coupling system in which ATP hydrolysis was coupled to NADH oxidation according to Lucena et al. (2012). NADH oxidation was monitored at 340 nm ($\varepsilon_{340}$ nm, pH 7.5, 6,200 $M^{-1}$ $cm^{-1}$) in a Hitachi (Tokyo, Japan) U-3000 spectrophotometer equipped with thermostatted cell holders. Standard conditions for measurement of ATPase activity in the gill microsomes were 50 mmol $L^{-1}$ HEPES buffer (pH 7.5) containing 2 mmol $L^{-1}$ ATP, 5 mmol $L^{-1}$ $MgCl_2$, 20 mmol $L^{-1}$ KCl, 50 mmol $L^{-1}$ NaCl, 0.3 mmol $L^{-1}$ NADH, 1.7 mmol $L^{-1}$ PEP, 82 µg PK (49 U), 110 µg LDH (94 U) and 20 µg alamethicin $\mu g^{-1}$ protein in a final volume of 1.0 mL.

To examine stimulation of the enzyme by $K^+$ and $NH_4^+$, we also used a GAPDH/PGK coupling system in which ATP hydrolysis was coupled to the reduction of $NAD^+$ at 340 nm according to Lucena et al. (2012) since neither enzyme is $K^+$-dependent. Standard conditions for measurement of ATPase activity in the gill microsomes using the GAPDH/PGK linked system were 50 mmol $L^{-1}$ triethanolamine buffer (pH 7.5), containing 2 mmol $L^{-1}$ ATP, 5 mmol $L^{-1}$ $MgCl_2$, 20 mmol $L^{-1}$ KCl, 50 mmol $L^{-1}$ NaCl, 2.86 mmol $L^{-1}$ $NAD^+$, 1 mmol $L^{-1}$ sodium phosphate, 2 mmol $L^{-1}$ G3P, 150 µg GAPDH (12 U), 20 µg PGK (9 U) and 20 µg alamethicin $\mu g^{-1}$ protein in a final volume of 1.0 mL.

The two coupling systems gave equivalent results with a difference of <10 %. The initial velocities were constant for at least 15 min provided that <5 % NADH ($NAD^+$) was oxidized (reduced); such measurements are considered to have been obtained under steady-state conditions. For each microsomal preparation, assay linearity was checked using samples containing 5–50 µg protein; total microsomal protein added to the cuvette always fell well within the linear range of the assay. Neither NADH, PEP, LDH, PK, $NAD^+$, G3P, PGK nor GAPDH was rate-limiting over the initial course of the assay; and no activity could be measured in the absence of NADH or $NAD^+$.

Controls without added enzyme were also included in each experiment to quantify nonenzymatic substrate hydrolysis. The reaction rate for each modulator concentration was estimated in duplicate aliquots from the same microsomal preparation, and the mean values were used to fit the respective saturation curve. Each saturation curve was repeated using three different microsomal homogenates.

ATP hydrolysis was also estimated in the presence of 3 mmol $L^{-1}$ ouabain to evaluate the ouabain-insensitive

activity. The difference in measured activity in the absence (total ATPase activity) or presence of ouabain (ouabain-insensitive activity) was considered to represent the ($Na^+$, $K^+$)-ATPase activity. ATPase activity was also assayed in the presence of alamethicin (0.5–22 μg $\mu g^{-1}$ protein) to evaluate the presence of sealed vesicles in the microsomal preparations. One enzyme unit is defined as the amount of enzyme that hydrolyzes 1.0 nmol of ATP per minute at 25 °C, and specific activity is given as nanomoles per minute per milligram protein.

### Continuous-Density Sucrose Gradient Centrifugation

An aliquot (3.5 mg) of the ATPase-rich gill microsomal fraction was layered into a 10–50 % (w/w) continuous-density sucrose gradient in 20 mmol $L^{-1}$ imidazole buffer, pH 6.8, and centrifuged at 180,000 × *g* and 4 °C for 3 h, using a PV50T2 Hitachi vertical rotor. Fractions (0.5 mL) collected from the bottom of the gradient were then assayed for total ATPase activity, ouabain-insensitive ATPase activity, protein concentration and refractive index.

### Measurement of Protein

Protein concentration was estimated according to Read and Northcote (1981), using BSA as the standard.

### SDS-PAGE and Western Blot Analysis

SDS-PAGE was performed in 5–20 % gels according to Laemmli (1970), using 2.5 and 100 μg protein/slot for protein staining and blotting analysis, respectively. After electrophoresis, the gel was split, one-half being stained with silver nitrate and the other electroblotted using a Hoefer SE200 system (Fisher Scientific, Holliston, MA) employing nitrocellulose membranes according to Towbin et al. (1979). The nitrocellulose membrane was incubated overnight at 4 °C in a 1:10 dilution (2.1 μg $mL^{-1}$) of the α-5 monoclonal antibody. After washing five times in 50 mmol $L^{-1}$ Tris–HCl buffer (pH 8.0) containing 150 mmol $L^{-1}$ NaCl and 0.1 % Tween 20, the membrane was incubated for 1 h at 25 °C in a 1:7,500 dilution of anti-mouse IgG, alkaline phosphatase conjugate. Specific antibody binding was developed in 100 mmol $L^{-1}$ Tris–HCl buffer (pH 9.5) containing 100 mmol $L^{-1}$ NaCl, 5 mmol $L^{-1}$ $MgCl_2$, 0.2 mmol $L^{-1}$ NBT and 0.8 mmol $L^{-1}$ BCIP. Immunoblots were scanned and imported as TIF files into a commercial software package (Kodak 1D 3.6; Kodak, Rochester, NY). Western blot analysis was repeated three times using different gill tissue preparations.

### Cellular Localization of Gill ($Na^+$, $K^+$)-ATPase

Fourth, right-side gills were dissected and incubated in a fixative solution containing 2 % *p*-formaldehyde in phosphate-buffered saline (PBS; in millimoles per liter, $Na_2HPO_4$ 10, $KH_2PO_4$ 2, NaCl 137, KCl 2.7, 290 mOsm $kg^{-1}$ $H_2O$), pH 7.4, for 1 h, then embedded in Optimal Cutting Temperature Compound. Cryosections 10-μm thick were taken transversely to the gill lamella long axis using a Microm HM 505E model Cryostat Microtome (Walldorf, Germany) at −25 °C and collected on gelatin-coated slides (Bloom 225). Cryosections were preincubated for 20 min with 100 mmol $L^{-1}$ glycine in PBS to mask free aldehyde groups and incubated for 10 min in blocking solution containing 1 % BSA and 0.1 % gelatin in PBS.

($Na^+$, $K^+$)-ATPase immunolocalization was performed using a mouse monoclonal IgG α-5 antibody raised against the chicken ($Na^+$, $K^+$)-ATPase α-subunit (Takeyasu et al. 1988). Droplets of primary antibody, diluted to 20 mg $mL^{-1}$ in PBS (1:1.75) were placed over the sections, which were incubated for 1 h at room temperature in a humid chamber. Negative control sections were incubated in blocking solution without the primary antibody. After washing six times for 5 min each in blocking solution to remove unbound antibodies, the sections were incubated for 45 min in droplets of a donkey anti-mouse IgG secondary antibody conjugated with Alexa-fluor 488 diluted 1:450 in PBS and then rinsed six times for 5 min each in PBS. To locate nuclei, sections were stained for 20 min with DAPI, diluted 1: 200 in PBS.

Sections were mounted in Fluoromount-G slide mounting medium with Knittel (Bielefeld, Germany) Starfrost slides and coverslips and observed and photographed using an Olympus (Melville, NY) BX-50 fluorescence microscope equipped with a SPOT RT3 25.4 2 Mb Slider camera (SPOT Imaging Solutions, Sterling Heights, MI). Sections were observed using differential interference contrast microscopy and employing excitation/emission wavelengths of 358/461 nm (DAPI) and 495/519 nm (Alexa-fluor 488).

### Estimation of Kinetic Parameters

The kinetic parameters $V_M$ (maximum velocity), $K_{0.5}$ (apparent dissociation constant of the enzyme–modulator complex), $K_M$ (Michaelis–Menten constant) and $n_H$ (Hill coefficient) for ATP hydrolysis were calculated using SigrafW software (Leone et al. 2005a). The curves provided are those that best fit the experimental data, given in the figures as mean values ± SEM derived from three different microsomal preparations. The kinetic parameters furnished in the tables are calculated values and represent the mean ± SD also derived from three different microsomal preparations. The apparent dissociation constant, $K_I$, of the enzyme–inhibitor complex was estimated as described by Lucena et al. (2012). SigrafW can be freely obtained from http://portal.ffclrp.usp.br/sites/fdaleone/downloads.

## Results

### Hemolymph Cation Concentrations

All hemolymph cation concentrations in the prawns when in freshwater were strongly hyperregulated above ambient values: 162.5 ± 3.2 mmol $Na^+$ $L^{-1}$ (250:1), 3.2 ± 0.1 mmol $K^+$ $L^{-1}$ (80:1), 15.6 ± 0.6 mmol $Ca^{2+}$ $L^{-1}$ (7.8:1) and 1.7 ± 0.6 mmol $Mg^{+2}$ $L^{-1}$ (8.1:1).

### Immunolocalization of the ($Na^+$, $K^+$)-ATPase α-Subunit

The epithelial architecture of *M. rosenbergii* gill lamellae, as seen in fixed frozen sections taken transversely to the lamella long axis, conforms to the typical palaemonid shrimp plan (Freire and McNamara 1995) (Fig. 1a). The pillar cell flanges underlie the fine cuticle on either side of the gill lamellae, their cell bodies abutting onto the continuous intralamellar septum (Fig. 1a), forming a system of narrow lacunae through which the hemolymph flows.

Immunofluorescence labeling using the anti-α5 antibody reveals the ($Na^+$, $K^+$)-ATPase α-subunit to be distributed predominantly, although irregularly, throughout the intralamellar septal cells (Fig. 1b). Staining was frequently more intense in the cytoplasm immediately facing the hemolymph space. No labeling was seen in the pillar cell bodies or flanges.

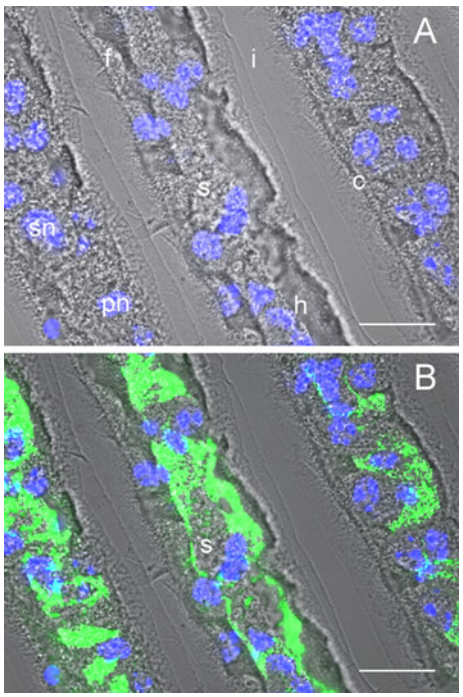


**Fig. 1** Immunolocalization of ($Na^+$, $K^+$)-ATPase α-subunit in *M. rosenbergii* gill lamellae. Frozen cross sections taken transversely to the long axes of gill lamellae incubated with mouse monoclonal IgG α-5 antibody raised against chicken ($Na^+$, $K^+$)-ATPase α-subunit. **a** Phase contrast/DAPI image showing typical lamellar structure in which the apical pillar cell flanges face the external medium below the fine cuticle, the pillar cell bodies abutting on the intralamellar septum bathed by the hemolymph. *c* cuticle, *f* pillar cell flange, *h* hemolymph space, *i* interlamellar space, *s* intralamellar septum, *pn* DAPI-stained pillar cell nuclei, *sn* intralamellar septal cell nuclei. **b** Immunofluorescence labeling (Alexa-fluor 488, 495/519 nm) showing distribution of the ($Na^+$, $K^+$)-ATPase α-subunit (*green*) located predominantly where the intralamellar septal cells face the hemolymph space and scattered throughout the septal cell cytoplasm. Pillar cell flanges and cell bodies are not labeled. *Scale bar* = 50 μm

## Characterization of the Gill Microsomal Fraction

Western blot analysis using the α-5 monoclonal antibody against the ($Na^+$, $K^+$)-ATPase α-subunit identified a single, low-intensity, immunoreactive band coincident with a 108-kDa protein band, suggesting a single α-subunit isoform (Fig. 2). Note that the ($Na^+$, $K^+$)-ATPase represents only a small proportion of the total protein content of the gill microsomal fraction.

Sucrose density gradient centrifugation analysis of gill microsomes is shown in Fig. 3. The main ($Na^+$, $K^+$)-ATPase activity peak (I) is coincident with the protein peak at ≈28 % sucrose (light fraction). A heavier fraction (II), showing lower ($Na^+$, $K^+$)-ATPase activity, elutes at ≈40 % sucrose.

### Characterization of Gill ($Na^+$, $K^+$)-ATPase Activity

The effect of increasing ATP concentrations on gill microsomal ($Na^+$, $K^+$)-ATPase activity is shown in Fig. 4. Under saturating $K^+$ (20 mmol $L^{-1}$), $Na^+$ (50 mmol $L^{-1}$) and $Mg^{2+}$ (5 mmol $L^{-1}$) concentrations, ATP hydrolysis followed a single curve over the range of $10^{-5}$ to $2 \times 10^{-3}$ mol $L^{-1}$. ATP was hydrolyzed with $V_M$ = 115.0 ± 2.3 nmol phosphate $min^{-1}$ $mg^{-1}$ and $K_{0.5}$ = 0.10 ± 0.01 mmol $L^{-1}$, obeying cooperative kinetics ($n_H$ = 1.5). At ATP concentrations as low as $10^{-5}$ mol $L^{-1}$, ($Na^+$, $K^+$)-ATPase activity was around 11 nmol phosphate $min^{-1}$ $mg^{-1}$; however, above $2 \times 10^{-3}$ mol $L^{-1}$, activity was inhibited by excess ATP (not shown). The ouabain-insensitive ATPase activity, corresponding to about 27 % of total ATPase activity, was also stimulated to ≈40 nmol phosphate $min^{-1}$ $mg^{-1}$ over the same ATP concentration range (inset a to Fig. 4). ATPase activity assayed in increasing alamethicin concentrations from 0.5 to 22 μg $μg^{-1}$ protein revealed sealed vesicles in the microsomal preparation since ($Na^+$, $K^+$)-ATPase activity was 79.6 nmol phosphate $min^{-1}$ $mg^{-1}$ and 150.2 nmol phosphate $min^{-1}$ $mg^{-1}$ in the absence and presence of alamethicin, respectively. Thus, to provide free access of substrate and ions to their respective sites on the enzyme molecule, all activity assays were performed after 20-min preincubation of a microsomal preparation with 20 μg alamethicin $μg^{-1}$ protein (inset b to Fig. 4).

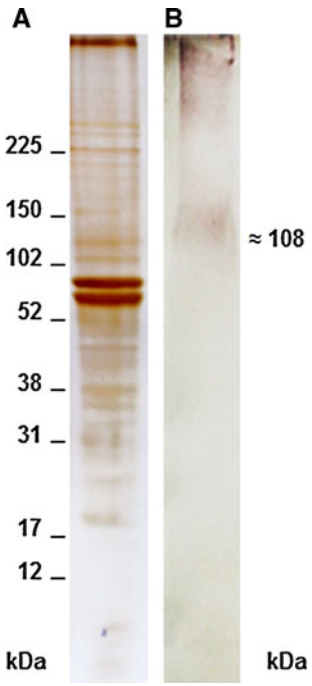


**Fig. 2** SDS-PAGE and Western blot analyses of gill microsomal fractions from *M. rosenbergii*. Electrophoresis was performed in a 5–20 % polyacrylamide gel. **a** Silver-stained gill microsomal protein. **b** Western blot analysis of gill microsomal protein using mouse monoclonal IgG α-5 antibody, identifying a single ($Na^+$, $K^+$)-ATPase α-subunit isoform at ≈108 kDa

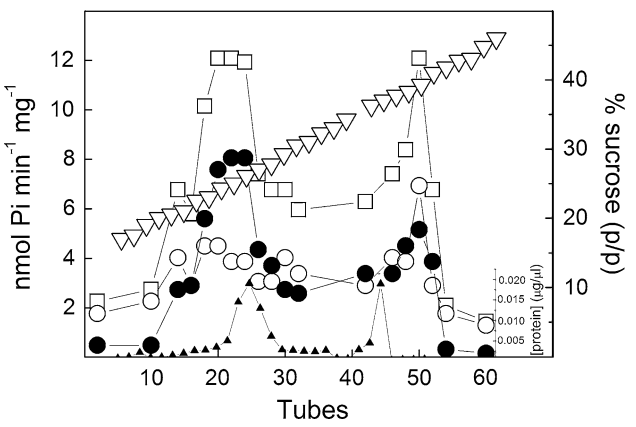


**Fig. 3** Sucrose density gradient centrifugation of the gill microsomal fraction from *M. rosenbergii*. An aliquot containing 3.5 mg of protein was layered into a 10–50 % (w/w) continuous sucrose density gradient in 20 mmol $L^{-1}$ imidazole buffer, pH 6.8, and centrifuged at 180,000×*g* for 3 h at 4 °C. Fractions (0.5 mL) were collected from the bottom of the gradient and analyzed for ($Na^+$, $K^+$)-ATPase activity (*filled circle*), protein concentration (*filled triangle*), sucrose concentration (*open inverted triangle*), total ATPase activity (*open square*) and ouabain-insensitive ATPase activity (*open cirle*)

The modulation by $Mg^{2+}$ and $Na^+$ of ($Na^+$, $K^+$)-ATPase activity is shown in Fig. 5. Under saturating ATP (2 mmol $L^{-1}$), $Na^+$ (50 mmol $L^{-1}$) and $K^+$ (20 mmol $L^{-1}$) concentrations, increasing $Mg^{2+}$ concentrations of 10–5 mmol $L^{-1}$ stimulated activity up to $V_M = 115.0 \pm 4.6$ nmol phosphate $min^{-1}$ $mg^{-1}$ with $K_{0.5} = 0.96 \pm 0.03$ mmol $L^{-1}$ (Fig. 5a). Cooperative effects ($n_H = 2.1$), suggesting multiple binding sites, were seen for the interaction of $Mg^{2+}$ with the enzyme. Activity was inhibited by excess free $Mg^{2+}$ (not shown). Ouabain-insensitive activity was also stimulated up to 42 nmol phosphate $min^{-1}$ $mg^{-1}$ over the same $Mg^{2+}$ concentration range (inset to Fig. 5a).

Under saturating ATP (2 mmol $l^{-1}$), $K^+$ (20 mmol $l^{-1}$) and $Mg^{2+}$ (5 mmol $l^{-1}$) concentrations, the $Na^+$ dependence of ($Na^+$, $K^+$)-ATPase activity was characterized by cooperative kinetics ($n_H = 2.1$) with $V_M = 110.0 \pm 3.3$ nmol phosphate $min^{-1}$ $mg^{-1}$ and $K_{0.5} = 1.3 \pm 0.03$ mmol $L^{-1}$ (Fig. 5b). A considerable fraction of the ($Na^+$, $K^+$)-ATPase activity (≈40 nmol phosphate $min^{-1}$ $mg^{-1}$) remained unaltered for $Na^+$ concentrations as low as $10^{-4}$ mol $L^{-1}$. As $Na^+$ concentration increased from $10^{-4}$ to $5 \times 10^{-2}$ mol $L^{-1}$, ouabain-insensitive ATPase activity was stimulated to maximum values of around 38 nmol phosphate $min^{-1}$ $mg^{-1}$ (inset to Fig. 5b), suggesting $Na^+$-stimulated ATPase activity in the microsomal preparation. This $Na^+$-stimulated activity represents ≈12 % of ouabain-insensitive ATPase activity.

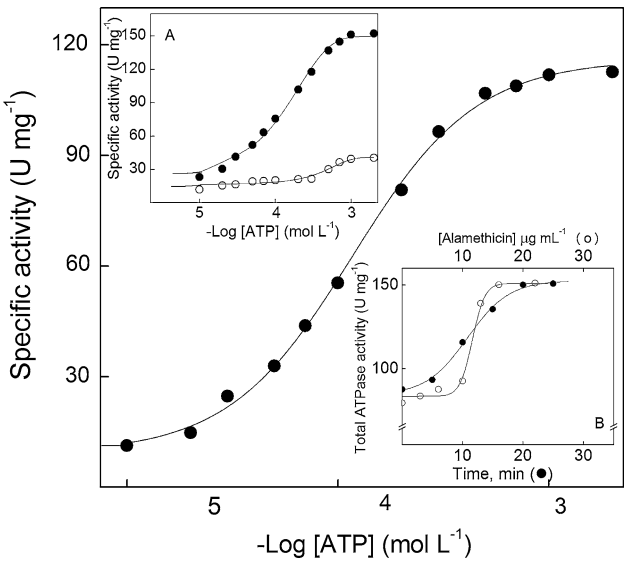


**Fig. 4** Effect of ATP concentration on ($Na^+$, $K^+$)-ATPase activity in the gill microsomal fraction from *M. rosenbergii*. Data are mean ± SEM ($n = 3$), obtained using duplicate aliquots containing 36.2 µg of protein from three different gill homogenates. Activity was assayed continuously at 25 °C in 50 mmol $L^{-1}$ HEPES buffer, pH 7.5, containing 5 mmol $L^{-1}$ $MgCl_2$, 50 mmol $L^{-1}$ NaCl, 20 mmol $L^{-1}$ KCl, 20 µg alamethicin/µg protein, 0.3 mmol $L^{-1}$ NADH, 1.7 mmol $L^{-1}$ PEP, PK (49 U) and LDH (94 U). *Inset a* Total ATPase activity (*filled circle*); ouabain-insensitive ATPase activity (*open cirle*). *Inset b* Time (*filled circle*) and concentration (*open cirle*) dependence of ($Na^+$, $K^+$)-ATPase activity on alamethicin

### Synergistic Stimulation by $K^+$ and $NH_4^+$ of Gill ($Na^+$, $K^+$)-ATPase Activity

The effect of $K^+$ and $NH_4^+$ on ATP hydrolysis by the microsomal ($Na^+$, $K^+$)-ATPase is shown in Fig. 6. Under saturating ATP (2 mmol $L^{-1}$), $Na^+$ (50 mmol $L^{-1}$) and $Mg^{2+}$ (5 mmol $L^{-1}$) concentrations and in the absence of $NH_4^+$, enzyme activity was stimulated by $K^+$ (from $10^{-4}$ to $10^{-1}$ mol $L^{-1}$) following Michaelis–Menten kinetics with $V_M = 120.0 \pm 2.4$ nmol phosphate $min^{-1}$ $mg^{-1}$ and $K_M = 2.74 \pm 0.08$ mmol $L^{-1}$ (Fig. 6a). Similarly to $Na^+$, ouabain-insensitive activity was stimulated around 12 % by increasing $K^+$ concentration over the same concentration range (inset to Fig. 6a). Negligible ($Na^+$, $K^+$)-ATPase activity (<7 nmol phosphate $min^{-1}$ $mg^{-1}$) was estimated at $K^+$ concentrations as low as $10^{-4}$ mol $L^{-1}$. However, when assayed at fixed $NH_4^+$ concentrations (2–20 mmol $L^{-1}$), synergistic stimulation by $K^+$ resulted in ≈22 % higher ($Na^+$, $K^+$)-ATPase activity ($V_M = 146.1 \pm 2.9$ nmol phosphate $min^{-1}$ $mg^{-1}$). Independently of $NH_4^+$ concentration, ATP hydrolysis obeyed site–site interaction kinetics (Table 1). Note that $NH_4^+$ ions are not displaced at high $K^+$ concentrations (20 mmol $L^{-1}$).

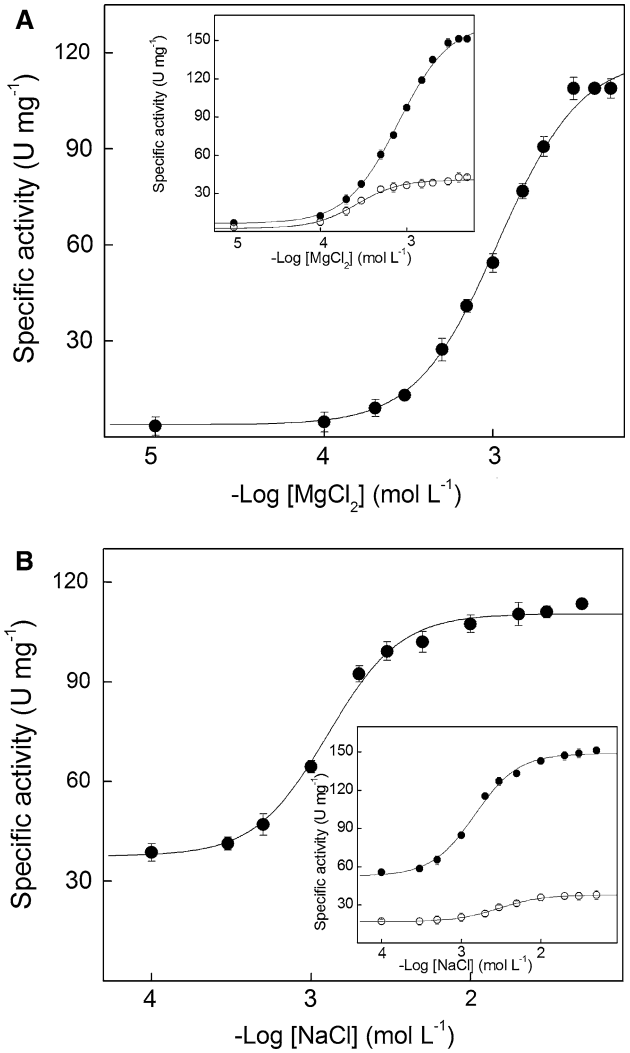


**Fig. 5** Effect of $Mg^{2+}$ and $Na^+$ on ($Na^+$, $K^+$)-ATPase activity in the gill microsomal fraction from *M. rosenbergii*. Data are mean ± SEM ($n = 3$), obtained using duplicate aliquots containing 36.2 µg of protein from three different gill homogenates. Activity was assayed continuously at 25 °C in 50 mmol $L^{-1}$ HEPES buffer, pH 7.5, containing 2 mmol $L^{-1}$ ATP, 20 mmol $L^{-1}$ KCl, 20 µg alamethicin/µg protein, 0.3 mmol $L^{-1}$ NADH, 1.7 mmol $L^{-1}$ PEP, PK (49 U) and LDH (94 U). **a** $Mg^{2+}$ in the presence of 50 mmol $L^{-1}$ NaCl. **b** $Na^+$ in the presence of 5 mmol $L^{-1}$ $MgCl_2$. *Insets* Total ATPase activity (*filled circle*); ouabain-insensitive ATPase activity (*open circle*)

Stimulation of ATP hydrolysis by $NH_4^+$ is shown in Fig. 6b. Under saturating ATP (2 mmol $L^{-1}$), $Na^+$ (50 mmol $L^{-1}$) and $Mg^{2+}$ (5 mmol $L^{-1}$) concentrations and in the absence of $K^+$, activity was stimulated by $NH_4^+$ obeying cooperative kinetics, with $V_M = 141.0 \pm 5.6$ nmol phosphate $min^{-1}mg^{-1}$ and $K_{0.5} = 1.9 \pm 0.04$ mmol $L^{-1}$. Interestingly, ouabain-insensitive activity of ($Na^+$, $K^+$)-ATPase was also stimulated around 12 % by increasing $NH_4^+$ concentration (inset to Fig. 6b). ($Na^+$, $K^+$)-ATPase activity of about 10 % (≈20 nmol phosphate $min^{-1}$ $mg^{-1}$) was found for $NH_4^+$ concentrations as low as $10^{-4}$ mol $L^{-1}$. Increasing $NH_4^+$ concentrations in the $K^+$-containing reaction media (1–20 mmol $L^{-1}$) also resulted in synergistic stimulation of ($Na^+$, $K^+$)-ATPase activity (≈26 %) with $V_M = 178.1 \pm 7.1$ nmol phosphate $min^{-1}$ $mg^{-1}$. Positive cooperativity was seen independently of $K^+$ concentration (Table 1). $K^+$ is not displaced by high $NH_4^+$ concentrations (20 mmol $L^{-1}$).

### Inhibition of Total ATPase Activity

The effects of ouabain and orthovanadate on total ATPase activity in the gill microsomal fraction are shown in Fig. 7. With 3 mmol $L^{-1}$ ouabain residual activity is around 13 nmol phosphate $min^{-1}$ $mg^{-1}$ (Fig. 7a). The inhibition pattern corresponds to that of a single inhibitor-binding site, and $K_I = 12.4 \pm 1.3$ µmol $L^{-1}$ (inset to Fig. 7a). Orthovanadate concentrations up to 50 µmol $L^{-1}$ also inhibit ($Na^+$, $K^+$)-ATPase activity around 75 % (Fig. 7b), which suggests that other P–ATPase types account for 36.5 ± 1.8 nmol phosphate $min^{-1}$ $mg^{-1}$. The $K_I$ for vanadate was 0.2 ± 0.04 µmol $L^{-1}$ (inset to Fig. 7b).

Additional inhibition studies were performed since total ATPase activity (151.2 ± 3.0 nmol phosphate $min^{-1}$ $mg^{-1}$) was partially inhibited (73 %) by ouabain. The remaining 27 % of microsomal ATPase activity corresponds to ATPases other than the ($Na^+$, $K^+$)-ATPase (Table 2). The substantial inhibition by aurovertin B plus ouabain is a strong indication of an $F_0F_1$–ATPase. The additional inhibitory effect of ethacrynic acid plus ouabain reveals $Na^+$- and/or $K^+$-ATPases. The kinetic data shown in the insets to Figs. 5a and 6 corroborate this idea. The lack of an additional inhibitory effect

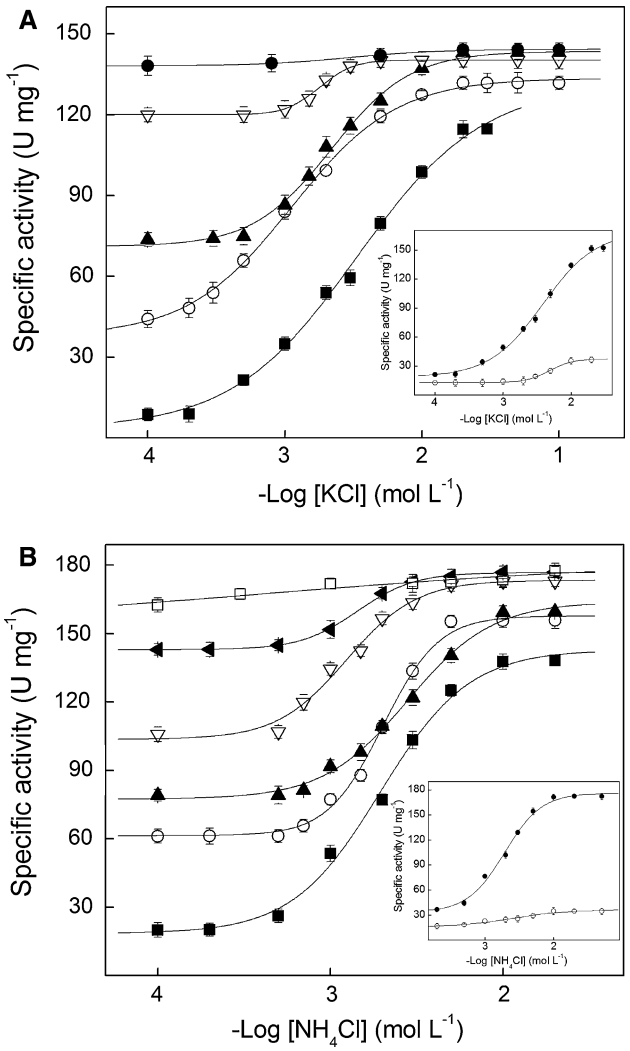


**Fig. 6** Effect of $K^+$ and $NH_4^+$ on ($Na^+$, $K^+$)-ATPase activity in the gill microsomal fraction of *M. rosenbergii*. Data are mean ± SEM ($n = 3$), obtained using duplicate aliquots containing 36.2 µg of protein from three different gill homogenates. Activity was assayed continuously at 25 °C in 50 mmol $L^{-1}$ HEPES buffer, pH 7.5, containing 2 mmol $L^{-1}$ ATP, 5 mmol $L^{-1}$ $MgCl_2$, 50 mmol $L^{-1}$ NaCl, 20 µg alamethicin/µg protein, 2.86 mmol $L^{-1}$ $NAD^+$, 1 mmol $L^{-1}$ sodium phosphate, 2 mmol $L^{-1}$ G3P, GAPDH (12 U) and PGK (9 U). **a** No $NH_4^+$ (*filled square*); 2 mmol $L^{-1}$ $NH_4^+$ (*open circle*); 3 mmol $L^{-1}$ $NH_4^+$ (*filled triangle*); 5 mmol $L^{-1}$ $NH_4^+$ (*open inverted triangle*); 20 mmol $L^{-1}$ $NH_4^+$ (*filled circle*). **b** No $K^+$ (*filled square*); 1 mmol $L^{-1}$ $K^+$ (*open circle*); 3 mmol $L^{-1}$ $K^+$ (*filled triangle*); 5 mmol $L^{-1}$ $K^+$ (*open inverted triangle*); 10 mmol $L^{-1}$ $K^+$ (*Back left pointing small triangle*); 20 mmol $L^{-1}$ $K^+$ (*open square*). *Insets* Total ATPase activity (*filled circle*); ouabain-insensitive ATPase activity (*open circle*)

by ouabain plus bafilomycin $A_1$ and orthovanadate plus bafilomycin $A_1$ or thapsigargin apparently excludes $V(H^+)$- and $Ca^{2+}$–ATPases, respectively.

Table 3 summarizes the kinetic parameters calculated for the modulation of ($Na^+$, $K^+$)–ATPase activity by ATP, $Mg^{2+}$, $Na^+$, $K^+$, $NH_4^+$, ouabain and orthovanadate.

## Discussion

Our extensive characterization of gill microsomal ($Na^+$, $K^+$)-ATPase activity in the giant freshwater prawn *M. rosenbergii* disclosed a single immunoreactive protein by Western blot analysis, suggesting that a single ($Na^+$, $K^+$)-ATPase α-subunit isoform is distributed into membrane fractions of different density. Immunolocalization showed the ($Na^+$, $K^+$)-ATPase to be distributed predominantly within the gill intralamellar septal cells and not in the pillar cells. Other important findings are the lack of a high-affinity ATP binding site, and the synergistic stimulation of enzyme activity, around 25 %, by $NH_4^+$ and $K^+$. We propose a model for $K^+/NH_4^+$ stimulation.

The ability of the Crustacea to become established in dilute media or freshwater depends mainly on their capacity to hyperregulate the ionic concentration of the extracellular fluid (Péqueux 1995; Lucu and Towle 2003; Kirschner 2004), a characteristic achieved through the coordinated activity of specialized ion transporting cells in the gills (Freire et al. 2003), renal organs and gut (Péqueux 1995; Weihrauch et al. 1999; Freire et al. 2008). The gills are the primary sites of ($Na^+$, $K^+$)-ATPase–driven ion uptake from the surrounding medium to the hemolymph in such organisms (Péqueux 1995; Towle 1997; Freire et al. 2008). Thus, understanding the modulation by substrate and ions of ($Na^+$, $K^+$)-ATPase activity in a diadromous species like *M. rosenbergii* provides a valuable perspective from which to better comprehend the biochemical adaptations underpinning the invasion of freshwater by this palaemonid shrimp group (Freire et al. 2003).

### Characterization of Gill Microsomal ($Na^+$, $K^+$)-ATPase Activity

Western blot analysis suggests that *M. rosenbergii* gill tissue contains a single α-subunit isoform of ($Na^+$, $K^+$)-ATPase, of ~108 kDa, typical of most crustaceans (Lucu and Flik 1999; Furriel et al. 2000; Towle and Weihrauch 2001; Masui et al. 2002, 2005; Belli et al. 2009; Garçon et al. 2007, 2009; Lucena et al. 2012). While α-subunit isoforms expressed in crustacean tissues are not well known, two different cDNAs encode the α-subunit (α1 and α2) from *Artemia franciscana* and a single cDNA has been cloned from *Homarus americanus*, *Callinectes sapidus* and other crabs (Lucu and Towle 2003; Weihrauch et al. 2004).

The two ($Na^+$, $K^+$)-ATPase activity peaks revealed by sucrose gradient centrifugation suggest that the α-subunit isoform in *M. rosenbergii* is distributed into membrane fractions of different density, as seen in *Callinectes ornatus* (Garçon et al. 2007, 2009), *Dilocarcinus pagei* (Furriel et al. 2010) and high salinity–acclimated *Clibanarius vittatus* (Lucena et al. 2012) but different from

**Table 1** Kinetic parameters for the synergistic stimulation by both $K^+$ and $NH_4^+$ of ($Na^+$, $K^+$)-ATPase activity in a microsomal fraction from the gill tissue of the giant freshwater prawn *M. rosenbergii*: data are mean ± SD ($n = 3$)

| [$K^+$] (mmol $L^{-1}$) | [$NH_4^+$] (mmol $L^{-1}$) | $V_M$ (nmol phosphate $min^{-1}$ $mg^{-1}$) | $K_{0.5}$ (mmol $L^{-1}$) | $n_H$ | $V_M/K_{0.5}$ ($\times 10^{-6}$) |
|---|---|---|---|---|---|
| Variable | 0 | 120.0 ± 4.8 | 2.7 ± 0.13 | 1.1 | 44.4 |
| Variable | 2 | 132.7 ± 4.0 | 1.3 ± 0.04 | 1.3 | 102.1 |
| Variable | 3 | 143.0 ± 2.9 | 2.3 ± 0.09 | 1.7 | 62.2 |
| Variable | 5 | 140.2 ± 5.6 | 1.8 ± 0.05 | 4.3 | 77.9 |
| Variable | 20 | 146.1 ± 2.9 | – | – | – |
| 0 | Variable | 141.0 ± 5.6 | 1.9 ± 0.04 | 1.8 | 74.2 |
| 1 | Variable | 157.7 ± 7.9 | 2.0 ± 0.06 | 2.9 | 78.8 |
| 3 | Variable | 163.2 ± 4.9 | 2.8 ± 0.08 | 1.9 | 58.3 |
| 5 | Variable | 162.3 ± 6.5 | 2.0 ± 0.06 | 1.9 | 81.1 |
| 10 | Variable | 176.7 ± 5.3 | 1.4 ± 0.05 | 2.8 | 126.2 |
| 20 | Variable | 178.1 ± 7.1 | – | – | – |

*Macrobrachium olfersi* (Furriel et al. 2000), fresh-caught *C. vittatus* (Gonçalves et al. 2006) and low salinity–acclimated *Callinectes danae* (Masui et al. 2009).

The residual ATPase activity seen after inhibition with 3.0 mmol $L^{-1}$ ouabain suggests that in addition to the ($Na^+$, $K^+$)-ATPase (73 %), the microsomal fraction contains other ATP-hydrolyzing enzymes (27 %). The substantial inhibition by ouabain plus aurovertin B is strong evidence for an $F_0F_1$–ATPase. Further, inhibition by ouabain plus orthovanadate together with inhibition by ouabain plus ethacrynic acid suggest the presence of $Na^+$- and $K^+$-ATPases, corroborated by the similar stimulation by $Na^+$, $K^+$ and $NH_4^+$ of ouabain-insensitive ATPase activity (insets to Figs. 5b, 6a, b). While ($Na^+$, $K^+$)-ATPase preparations from crustacean gill tissues are usually contaminated by neutral (Lovett et al. 1994) and/or acid and alkaline phosphatases (Reddy and Rao 1990) and $Ca^{2+}$-ATPase (Morris and Greenaway 1992; Flik et al. 1994), we believe that the presence of these different ATPase types in the gill tissue not only is species-specific but also depends on salinity acclimation (Leone et al. 2010). The apparent lack of a V($H^+$)ATPase activity in the gill microsomal preparation from *M. rosenbergii* may derive from the fact that phosphohydrolytic activity by the V-ATPase lies below the sensitivity of the assay method at the total protein concentration employed. Alternatively, the V-ATPase protein itself might not be incorporated into the microsomal fraction or is negligible compared to the ($Na^+$, $K^+$)-ATPase.

## ($Na^+$, $K^+$)-ATPase Activity

The specific activity of about 115 U $mg^{-1}$ estimated for *M. rosenbergii* gill ($Na^+$, $K^+$)-ATPase is lower than those for *Macrobrachium amazonicum* and *M. olfersi* (Furriel et al. 2000; Santos et al. 2007; Leone et al. 2012). ($Na^+$, $K^+$)-ATPase specific activities for total homogenates and microsomal gill tissue fractions from different crustacean species vary widely (Lucu and Towle 2003; Leone et al. 2005b). For the genus *Macrobrachium*, specific activities range from 70 to 100 U $mg^{-1}$ for gill homogenates (Moretti et al. 1991; Proverbio et al. 1991) and from 120 to 700 U $mg^{-1}$ for microsomal fractions (Stern et al. 1984; Lima et al. 1997; Furriel et al. 2000). The lower specific activity of the *M. rosenbergii* gill microsomal fraction compared to *M. olfersi* and *M. amazonicum* (Furriel et al. 2000; Santos et al. 2007; Leone et al. 2012) together with the lower relative ($Na^+$, $K^+$)-ATPase α-subunit content revealed in Western blot analyses suggest the expression of a different α-subunit isoform in *M. rosenbergii*. Differences in specific activity among crustacean ($Na^+$, $K^+$)-ATPases may result from the expression of different α-subunit isoforms of the enzyme that thus exhibit different kinetic properties (Therien et al. 1996; Blanco and Mercer 1998; Sweeney and Klip 1998; Crambert et al. 2000; Geering 2001; Segall et al. 2001; Lopez et al. 2002). Membrane and/or posttranslational factors also may participate in enzyme regulation (Sweadner 1989; Levenson 1994; Therien et al. 1996; Lopez et al. 2002).

The single family of ATP binding sites found for *M. rosenbergii* ($Na^+$, $K^+$)-ATPase resembles those of *M. olfersi* (Furriel et al. 2000), *C. ornatus* (Garçon et al. 2007, 2009), *C. danae* (Masui et al. 2009) and *C. sapidus* (Neufeld et al. 1980). However, this single pattern for ATP stimulation of ($Na^+$, $K^+$)-ATPase activity contrasts with high- and low-affinity ATP binding sites reported for acclimated *C. danae* (Masui et al. 2002), *C. vittatus* (Gonçalves et al. 2006; Lucena et al. 2012), *M. amazonicum* (Santos et al. 2007) and *D. pagei* (Furriel et al. 2010). The vertebrate enzyme displays high-affinity (E1-ATP site with $K_M$ of 0.1–1.0 mmol $L^{-1}$) and low-affinity (E2-ATP site with $K_M$ of 0.01–0.2 mmol $L^{-1}$) binding sites (Glynn 1985; Ward and Cavieres 1998; Taniguchi et al. 2001). While the characterization of ATP binding sites on the ($Na^+$, $K^+$)-ATPase is still controversial (Beaugé et al. 1997; Martin and Sachs 2000; Krumscheid et al. 2004),

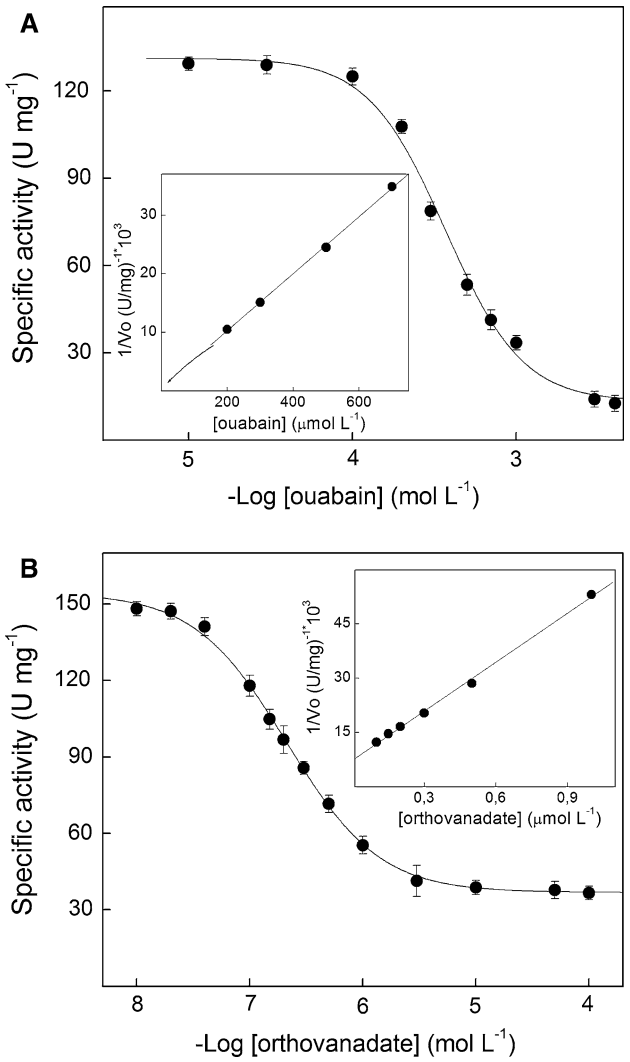


**Fig. 7** Effect of ouabain and orthovanadate on total ATPase activity in the gill microsomal fraction of *M. rosenbergii*. Data are mean ± SEM ($n = 3$), obtained using duplicate aliquots containing 36.2 µg of protein from three different gill homogenates. Activity was assayed continuously at 25 °C in 50 mmol $L^{-1}$ HEPES buffer, pH 7.5, containing 2 mmol $L^{-1}$ ATP, 5 mmol $L^{-1}$ $MgCl_2$, 50 mmol $L^{-1}$ NaCl, 20 mmol $L^{-1}$ KCl, 20 µg alamethicin/µg protein, 0.3 mmol $L^{-1}$ NADH, 1.7 mmol $L^{-1}$ PEP, PK (49 U) and LDH (94 U). **a** Ouabain. **b** Orthovanadate. *Inset* Dixon plot for estimation of $K_I$ in which $v_c$ is the reaction rate corresponding to ($Na^+$, $K^+$)-ATPase activity

recent crystallographic data (Morth et al. 2007; Shinoda et al. 2009; Ogawa et al. 2009) reveal only a single ATP binding site in the N-domain that exhibits low and high affinities in the E2 and E1 conformations, respectively (Chourasia and Sastry 2012). The cytoplasmic loop between the α-subunit transmembrane helices 4 and 5, containing the P- and N-domains, exhibits only a single ATP binding pocket (Morth et al. 2007; Shinoda et al. 2009; Ogawa et al. 2009).

In the absence of $Mg^{2+}$, the *M. rosenbergii* ($Na^+$, $K^+$)-ATPase does not hydrolyze ATP (see Glynn 1985; Garçon et al. 2009; Lucena et al. 2012). The affinity ($K_{0.5} = 0.96 \pm 0.03$ mmol $L^{-1}$) for $Mg^{2+}$ is very similar to that for *M. olfersi* (Furriel et al. 2000). Euryhaline crabs (Corotto and Holliday 1996; Holliday 1985; D'Orazio and Holliday 1985; Neufeld et al. 1980) and *M. amazonicum* (Santos et al. 2007) exhibit higher $K_{0.5}$ values. The inhibition by excess $Mg^{2+}$ is particularly interesting: while such inhibition may result from binding to a second inhibitory site on the enzyme (Pedemonte and Beaugé 1983), the physiological significance of enzyme inhibition at high $Mg^{2+}$ titers is unclear. Free $Mg^{2+}$ concentrations above 3 mmol $L^{-1}$ apparently shift the equilibrium toward the E2 enzyme form (Castro and Farley 1979; Robinson 1982; Tribuzy et al. 2002), decreasing affinity for ATP at the rate-limiting step of the reaction cycle as a consequence of $Mg^{2+}$ binding to the E2 K form (Forbush 1987; Pedemonte and Beaugé 1983; Fontes et al. 1992).

Distinct ($Na^+$, $K^+$)-ATPase α-subunit isoforms have different apparent affinities for $Na^+$ and $K^+$ when ATP is the substrate (Blanco and Mercer 1998; Sweeney and Klip 1998; Crambert et al. 2000; Segall et al. 2001; Lopez et al. 2002). These differences depend on organism and tissue, membrane factors and posttranslational modifications (Beaugé et al. 1997; Geering 2001) and have been attributed to kinetic differences in the ability of each α-isoform to displace the E1–E2 equilibrium and/or to associate with distinct β-subunits present in the different tissues (Therien et al. 1996; Segall et al. 2001). The affinity of *M. rosenbergii* gill ($Na^+$, $K^+$)-ATPase for $Na^+$ is similar to that for well-adapted freshwater Crustacea (Harris and Bayliss 1988; Lucu and Towle 2003; Leone et al. 2005b) but three to fivefold higher than that of *M. olfersi* (Furriel et al. 2000), *C. danae* (Masui et al. 2002), *C. vittatus* (Gonçalves et al. 2006; Lucena et al. 2012), *M. amazonicum* (Santos et al. 2007) and *C. ornatus* (Garçon et al. 2009). Estuarine crustaceans show comparable $K_{0.5}$ values (Specht et al. 1997; Lucu and Towle 2003), while marine osmoconformers exhibit seven to tenfold higher values (Leone et al. 2005b).

Stimulation of crustacean gill ($Na^+$, $K^+$)-ATPase by $K^+$ is similar among different species, independently of the biotope inhabited. The apparent affinity of the ($Na^+$, $K^+$)-ATPase for $K^+$ is about twofold lower in *M. rosenbergii* than in *C. danae* (Masui et al. 2002), *C. ornatus* (Garçon et al. 2007, 2009), *M. amazonicum* (Santos et al. 2007), *M. olfersi* (Furriel et al. 2000) and *C. vittatus* (Gonçalves et al. 2006; Lucena et al. 2012). The Hill coefficient ($n_H = 1.1$) for enzyme stimulation by $K^+$ is similar to the Michaelis–Menten behavior of the ($Na^+$, $K^+$)-ATPase from *M. olfersi* (Furriel et al. 2000), *C. vittatus* (Gonçalves et al. 2006), *M. amazonicum* (Santos et al. 2007; Leone et al. 2012), *Uca pugnax* (Holliday 1985) and *Uca pugilator* (D'Orazio and Holliday 1985) but contrasts with the multiple $K^+$ binding sites reported

**Table 2** Effect of various inhibitors on ATPase activity in a microsomal fraction from the gill tissue of the giant freshwater prawn *M. rosenbergii*: data are mean ± SD ($n = 3$)

| Inhibitor | $V_M$ (nmol phosphate $min^{-1}$ $mg^{-1}$) | % $V_M$ | Specific ATPase activity (%) | ATPase type likely present |
|---|---|---|---|---|
| Control | 151.2 ± 3.0 | 100 | – | |
| Ouabain (3 mmol $L^{-1}$) | 40.0 ± 2.0 | 26.5 | 73.5 | $Na^+$, $K^+$ |
| Orthovanadate (50 µmol $L^{-1}$) | 21.4 ± 1.1 | 14.2 | 85.8 | $Na^+$, $K^+$ and P |
| Orthovanadate (50 µmol $L^{-1}$) + bafilomycin $A_1$ (0.4 µmol $L^{-1}$) | 21.9 ± 1.5 | 14.5 | ≈0 | $V(H^+)$ |
| Ouabain (3 mmol $L^{-1}$) + orthovanadate (50 µmol $L^{-1}$) | 24.6 ± 0.5 | 16.3 | 10.2 | P |
| Ouabain (3 mmol $L^{-1}$) + ethanol (20 µL $mL^{-1}$) | 39.9 ± 1.9 | 26.5 | – | – |
| Ouabain (3 mmol $L^{-1}$) + DMSO (20 µg $mL^{-1}$) | 39.9 ± 1.6 | 26.5 | – | – |
| Ouabain (3 mmol $L^{-1}$) + aurovertin B (10 µmol $L^{-1}$) | 11.6 ± 0.6 | 7.6 | 18.9 | $F_0F_1$ |
| Ouabain (3 mmol $L^{-1}$) + bafilomycin $A_1$ (0.4 µmol $L^{-1}$) | 38.7 ± 1.5 | 25.6 | ≈0 | $V(H^+)$ |
| Ouabain (3 mmol $L^{-1}$) + Ethacrynic acid (2 mmol $L^{-1}$) | 11.1 ± 1.6 | 7.3 | 19.2 | $Na^+$ or $K^+$ |
| Ouabain (3 mmol $L^{-1}$) + Theophylline (5 mmol $L^{-1}$) | 17.7 ± 0.5 | 11.7 | 14.8 | Neutral phosphatases |
| Ouabain (3 mmol $L^{-1}$) + Thapsigargin (0.5 µmol $L^{-1}$) | 39.1 ± 0.8 | 25.7 | ≈0 | $Ca^{2+}$ |

**Table 3** Kinetic parameters for the stimulation by ATP, $Mg^{2+}$, $Na^+$, $K^+$ and $NH_4^+$ and inhibition by ouabain and orthovanadate of ($Na^+$, $K^+$)–ATPase activity in a microsomal fraction of gill tissue from the giant freshwater prawn *M. rosenbergii*: data are mean ± SD ($n = 3$)

| Modulator | $V_M$ (nmol phosphate $min^{-1}$ $mg^{-1}$) | $K_{0.5}$ or $K_M$ (mmol $L^{-1}$) | $n_H$ | $K_I$ (µmol $L^{-1}$) | $V_M/K_M$ ($\times 10^{-6}$) |
|---|---|---|---|---|---|
| ATP | 115.0 ± 2.3 | 0.10 ± 0.01 | 1.5 | – | 1,045 |
| $Mg^{2+}$ | 115.0 ± 4.6 | 0.96 ± 0.03 | 2.1 | – | 120 |
| $Na^+$ | 110.0 ± 3.3 | 1.30 ± 0.03 | 2.1 | – | 85 |
| $K^+$ | 120.0 ± 2.4 | 2.74 ± 0.08 | 1.1 | – | 44 |
| $NH_4^+$ | 141.0 ± 5.6 | 1.90 ± 0.04 | 1.8 | – | 74 |
| Ouabain | – | – | – | 12.4 ± 1.3 | – |
| Orthovanadate | – | – | – | 0.2 ± 0.04 | – |

for *C. danae* (Masui et al. 2002) and 45 ‰–acclimated *C. vittatus* (Lucena et al. 2012) gill enzymes.

## Synergistic Stimulation by $K^+$ and $NH_4^+$ of ($Na^+$, $K^+$)-ATPase Activity

$NH_4^+$ stimulated enzyme activity to up to 17 % greater values than did $K^+$, as also seen in vertebrate (Robinson 1970) and crustacean (Masui et al. 2002; Furriel et al. 2004; Leone et al. 2005b; Santos et al. 2007; Lucena et al. 2012) gill enzymes. $NH_4^+$ can substitute for $K^+$ in sustaining ATP hydrolysis by ($Na^+$, $K^+$)-ATPase from various sources including the crustacean gill, although with a lower affinity (Holliday 1985; Furriel et al. 2000, 2004, 2010; Masui et al. 2002; Gonçalves et al. 2006; Garçon et al. 2007; Santos et al. 2007; Lucena et al. 2012), owing to the fact that the two hydrated ions have very similar ionic radii (Knepper et al. 1989). Like $K^+$, $NH_4^+$ is actively transported by the vertebrate enzyme (Wall 1996) and can substitute for $K^+$ in $Na^+$ transport in *C. sapidus* (Towle and Holleland 1987).

The synergistic stimulation by $K^+$ and $NH_4^+$ of the crustacean gill ($Na^+$, $K^+$)-ATPase, first described in *C. danae* (Masui et al. 2002, 2005), appears to be a phenomenon widespread among the decapod Crustacea (Furriel et al. 2000, 2010; Gonçalves et al. 2006; Garçon et al. 2007, 2009; Santos et al. 2007; Lucena et al. 2012). The additional increase of ≈25 % seen in $V_M$ with $K^+$ plus $NH_4^+$ suggests distinct binding sites on the *M. rosenbergii* enzyme that are occupied simultaneously by these two ions. While each ion stimulates enzyme activity in the presence of the other, $K_{0.5}$ apparently remains unaffected (see Fig. 6, Table 1). $NH_4^+$ binding seems to induce conformational changes that affect $V_M$ with minor effects on $K_{0.5}$ (Gonçalves et al. 2006; Garçon et al. 2009; Lucena et al. 2012). Our findings also disclose that neither $K^+$ nor $NH_4^+$ can displace the other from its respective binding sites.

With few exceptions, crustaceans are ammoniotelic (Weihrauch et al. 1998, 1999). Most ammonia excretion occurs via the gills (Weihrauch et al. 1999), and <2 % is eliminated via the urine in *C. sapidus* (Cameron and Batterton 1978). Much of the ammonia content is excreted as

$NH_4^+$ (Weihrauch et al. 1998, 1999), and the sensitivity of active transepithelial $NH_4^+$ ion fluxes to basolateral ouabain strongly suggests involvement of ($Na^+$, $K^+$)-ATPase (Weihrauch et al. 1998, 1999; Lucu et al. 1989). According to Weihrauch et al. (1998), basolateral ($Na^+$, $K^+$)-ATPase participates directly in translocation of $NH_4^+$ from the hemolymph into the epithelial cells. Increased intracellular $NH_4^+$ then generates a gradient across the apical membrane that drives the outward flux of $NH_4^+$ from the gill epithelial cells via an apical $Na^+/NH_4^+$ antiporter.

Ambient ammonia in the aquatic environment is usually low as a consequence of bacterial nitrification of ammonia to nitrite and nitrate followed by absorption by autotrophs (Weihrauch et al. 1999). In unpolluted, oxygenated freshwater, $NH_4^+$ concentrations rarely exceed 5 mmol $L^{-1}$ (Koroleff 1983), in contrast to hemolymph concentrations of $\approx$100 mmol $L^{-1}$ in various brachyuran species adapted to different salinities (Weihrauch et al. 1999). In palaemonids, like *M. rosenbergii* and *M. olfersi*, oxygen consumption is maximum in freshwater or low salinity, partially reflecting augmented energy expenditure to maintain a hyperosmotic hemolymph (Stern et al. 1984; McNamara and Moreira 1987; Herrera and Ramírez 1993). The predominant energy-consuming phenomena include accelerated oxidative deamination of free amino acids, which results in higher hemolymph ammonia concentrations and increased ammonia excretion rates (Stern et al. 1984; McNamara and Moreira 1987; Herrera and Ramírez 1993). Hemolymph $NH_4^+$, translocated into the cytosol of the gill epithelial cells by basolateral ($Na^+$, $K^+$)-ATPase, can be exchanged for $Na^+$ via an apical $Na^+/NH_4^+$ antiporter, thus contributing to $Na^+$ uptake (Mangum and Towle 1977; Armstrong et al. 1981).

In conclusion, although $NH_4^+$ excretion and active ion uptake may not be directly coupled in euryhaline crabs (Weihrauch et al. 1999), the synergistic stimulation of *M. rosenbergii* gill ($Na^+$, $K^+$)-ATPase by $NH_4^+$ and $K^+$, as seen in other crustacean gill ($Na^+$, $K^+$)-ATPases (Masui et al. 2002; Gonçalves et al. 2006; Garçon et al. 2007, 2009; Santos et al. 2007; Furriel et al. 2010; Lucena et al. 2012) may constitute a physiologically relevant, biochemical mechanism underlying osmoregulatory and excretory processes in the Crustacea.

**Acknowledgments** This work constitutes part of a Ph.D. thesis by Juliana L. França and was supported by research grants from the Fundação de Amparo à Pesquisa do Estado de São Paulo (FAPESP), Conselho de Desenvolvimento Científico e Tecnológico (CNPq), CAPES (Coordenação de Aperfeiçoamento de Pessoal de Nível Superior) and Instituto Nacional de Ciência e Tecnologia (INCT) Adapta/Fundação de Amparo à Pesquisa do Estado do Amazonas (FAPEAM, 573976/2008-2). Juliana L. França and Malson N. Lucena received scholarships from CNPq and FAPESP, respectively. Daniela P. Garçon and Marcelo R. Pinto received post-doctoral scholarships from FAPESP and CNPq, respectively. Francisco A. Leone and John C. McNamara received research scholarships from CNPq. This laboratory (Francisco A. Leone) is integrated with the Amazon Shrimp Network (Rede de Camarão da Amazônia) and with ADAPTA (Centro de Estudos de Adaptações da Biota Aquática da Amazônia).

## References

Armstrong DA, Strange K, Crowe J, Knight A, Simmons M (1981) High salinity acclimation by the prawn *Macrobrachium rosenbergii*—uptake of exogenous ammonia and changes in endogenous nitrogen compounds. Biol Bull 160:349–365

Augusto A, Greene LJ, Laure HJ, McNamara JC (2007) The ontogeny of isosmotic intracellular regulation in the diadromous freshwater palaemonid shrimps *Macrobrachium amazonicum* and *M. olfersi* (Crustacea Decapoda). J Crust Biol 27:626–634

Beaugé LA, Gadsby DC, Garrahan PJ (1997) Na/K-ATPase and related transport ATPases: structure mechanism and regulation. Ann N Y Acad Sci 834:1–694

Belli NM, Faleiros RO, Firmino KCS, Masui DC, Leone FA, McNamara JC, Furriel RPM (2009) NaK-ATPase activity and epithelial interfaces in gills of the freshwater shrimp *Macrobrachium amazonicum* (Decapoda: Palaemonidae). Comp Biochem Physiol A 152:431–439

Blanco G, Mercer RW (1998) Isozymes of the ($Na^+K^+$)-ATPase: heterogeneity in structure diversity in function. Am J Physiol Renal Physiol 44:F633–F650

Cameron JN, Batterton CV (1978) Antennal gland function in the freshwater crab *Callinectes sapidus*: water electrolyte acid-base and ammonia excretion. J Comp Physiol B 123:143–148

Castro J, Farley RA (1979) Proteolytic fragmentation of the catalytic subunit of sodium and potassium adenosine triphosphatase. J Biol Chem 254:2221–2228

Chen JC, Kou CT (1996) Nitrogenous excretion in *Macrobrachium rosenbergii* at different pH levels. Aquaculture 144:155–164

Chourasia M, Sastry N (2012) The nucleotide inhibitor and cation binding sites of P-type II ATPases. Chem Biol Drug Design 79:617–627

Corotto FS, Holliday CW (1996) Branchial NaK-ATPase and osmoregulation in the purple shore crab *Hemigrapsus nudus* (Dana). Comp Biochem Physiol A 113:361–368

Crambert G, Hasler U, Beggah AT, Yu C, Modyanov NN, Horisberger JD, Lelievre L, Geering K (2000) Transport and pharmacological properties of nine different human NaK-ATPase isozymes. J Biol Chem 275:1976–1986

D'Orazio SE, Holliday CW (1985) Gill NaK-ATPase and osmoregulation in the sand fiddler crab *Uca pugilator*. Physiol Zool 58:364–373

Faleiros RO, Goldman MHS, Furriel RPM, McNamara JC (2010) Differential adjustment in gill $Na^+/K^+$- and V-ATPase activities and transporter mRNA expression during osmoregulatory acclimation in the cinnamon shrimp *Macrobrachium amazonicum* (Decapoda, Palaemonidae). J Exp Biol 15:3894–3905

Flik G, Verbost PM, Atsma W, Lucu C (1994) Calcium transport in gill plasma membranes of the crab *Carcinus maenas*: evidence for carriers driven by ATP and a $Na^+$ gradient. J Exp Biol 195:109–122

Fontes CFL, Barrabin H, Scofano HM, Norby JG (1992) The role of $Mg^{2+}$ and $K^+$ in the phosphorylation of $Na^+K^+$-ATPase by ATP in the presence of dimethylsulfoxide but in the absence of $Na^+$. Biochim Biophys Acta 1104:215–225

Forbush B III (1987) Rapid release of $^{42}K$ and $^{86}Rb$ from an occluded state of the NaK-pump in the presence of ATP or ADP. J Biol Chem 262:11104–11115

Freire CA, Cavassin F, Rodrigues EN, Torres AH, McNamara JC (2003) Adaptive patterns of osmotic and ionic regulation, and the

invasion of fresh water by the palaemonid shrimps. Comp Biochem Physiol A 136:771–778

Freire CA, McNamara JC (1995) Fine structure of the gills of the freshwater shrimp *Macrobrachium olfersii* (Decapoda): effect of acclimation to high salinity medium and evidence for involvement of the lamellar septum in ion uptake. J Crustacean Biol 15:103–116

Freire CA, Onken H, McNamara JC (2008) A structure–function analysis of ion transport in crustacean gills and excretory organs. Comp Biochem Physiol A 151:272–304

Furriel RPM, McNamara JC, Leone FA (2000) Characterization of ($Na^+$, $K^+$)-ATPase in gill microsomes of the freshwater shrimp Macrobrachium olfersi. Comp Biochem Physiol B 126:303–315

Furriel RPM, Masui DC, McNamara JC, Leone FA (2004) Modulation of gill ($Na^+K^+$)-ATPase activity by ammonium ions: putative coupling of nitrogen excretion and ion uptake in the freshwater shrimp *Macrobrachium olfersi*. J Exp Zool 301A:63–74

Furriel RPM, Firmino KCS, Masui DC, Faleiros RO, Torres AH, McNamara JC (2010) Structural and biochemical correlates of $Na^+$, $K^+$-ATPase driven ion uptake across the posterior epithelium of the true freshwater crab Dilocarcinus pagei (Brachyura Trichodactylidae). J Exp Zool 313A:508–523

Garçon DP, Masui DC, Mantelatto FLM, McNamara JC, Furriel RPM, Leone FA (2007) $K^+$ and $NH_4^+$ modulate gill ($Na^+$ $K^+$)-ATPase activity in the blue crab *Callinectes ornatus*: fine tuning of ammonia excretion. Comp Biochem Physiol A 147:145–155

Garçon DP, Masui DC, Mantelatto FLM, McNamara JC, Furriel RPM, Leone FA (2009) Hemolymph ionic regulation e adjustments in gill ($Na^+$, $K^+$)-ATPase activity during salinity acclimation in the swimming crab Callinectes ornatus (Decapoda Brachyura). Comp Biochem Physiol A 154:44–55

Garty H, Karlish SJD (2006) Role of FXYD proteins in ion transport. Annu Rev Physiol 68:431–459

Geering K (2001) The functional role of β-subunits in oligomeric P-type ATPases. J Bioenerg Biomembr 33:425–438

Geering K (2008) Functional roles of NaK-ATPase subunits. Curr Opin Nephrol Hypertens 17:526–532

Genovese G, Luchetti CG, Luquet CM (2004) $Na^+/K^+$-ATPase activity in gill ultrastructure in the hyper- hypo-regulating crab *Neohelice granulatus* acclimated to dilute normal in concentrated seawater. Mar Biol 144:111–118

Glynn IM (1985) The ($Na^+K^+$)-transporting adenosine triphosphatase. In: Martonosi AN (ed) The enzymes of biological membranes, vol 3. Plenum, New York, pp 35–114

Gonçalves RR, Masui DC, McNamara JC, Mantelatto FLM, Garçon DP, Furriel RPM, Leone FA (2006) A kinetic study of the gill ($Na^+$ $K^+$)-ATPase and its role in ammonia excretion in the intertidal hermit crab *Clibanarius vittatus*. Comp Biochem Physiol A 145:346–356

Harris RR, Bayliss D (1988) Gill ($Na^+K^+$)-ATPases in decapod crustaceans: distribution and characteristics in relation to $Na^+$ regulation. Comp Biochem Physiol A 90:303–308

Herrera FD, Ramírez FB (1993) Efecto de la salinidad sobre el consumo deoxigeno y la excreción de amônio de *Macrobrachium rosenbergii* (Crustacea: Palaemonidae). Rev Biol Trop 41:239–243

Holliday CW (1985) Salinity-induced changes in gill NaK-ATPase activity in the mud fiddler crab *Uca pugnax*. J Exp Zool 233:199–208

Horisberger JD (2004) Recent insights into the structure and mechanism of the sodium pump. Physiology 19:377–388

Jasmani S, Jayasankar V, Wilder MN (2008) Carbonic anhydrase and Na/K-ATPase activities at different molting stages of the giant freshwater prawn *Macrobrachium rosenbergii*. Fish Sci 74:488–493

Kaplan JH (2002) Biochemistry of NaK-ATPase. Annu Rev Biochem 71:511–535

Kirschner LB (1979) Control of the extracellular fluid osmolality: control mechanisms in crustaceans and fishes. In: Gilles R (ed) Mechanisms of osmoregulation in animals. Wiley, New York, pp 157–222

Kirschner LB (2004) The mechanism of sodium chloride uptake in hyperregulating aquatic animals. J Exp Biol 207:1439–1452

Knepper MA, Packer R, Good DW (1989) Ammonium transport in the kidney. Physiol Rev 69:179–249

Koroleff F (1983) Determination of ammonia. In: Grasshoff K, Ehrhart M, Kremling K (eds) Methods of seawater analysis. Chemie, Weinheim, pp 150–151

Krumscheid R, Ettrich R, Sovova Z, Susankova K, Lansky Z, Hofbauerova K, Linnertz H, Teisinger J, Amler E, Schoner W (2004) The phosphatase activity of the isolated H-4–H-5 loop of Na K ATPase residues outside its ATP binding site. Eur J Biochem 271:3923–3936

Laemmli UK (1970) Cleavage of structural proteins during assembly of head of bacteriophage-T4. Nature 227:680–685

Leone FA, Baranauskas JA, Furriel RPM, Borin IA (2005a) An easy-to-use program for fitting enzyme kinetic data. Biochem Mol Biol Ed 33:399–403

Leone FA, Furriel RPM, McNamara JC, Mantelatto FLM, Masui DC, Rezende LA, Gonçalves RR, Garçon DP (2005b) ($Na^+K^+$)-ATPase from crustacean gill microsomes: a molecular marker to evaluate adaptation to biotopes of different salinity. Trends Comp Biochem Physiol 11:1–15

Leone FA, Masui DC, Garçon DP, Fontes CFL, McNamara JC (2010) Avoiding traps and pitfalls in enzyme inhibition studies: the crustacean gill ($Na^+K^+$)-ATPase paradigm. Trends Cell Mol Biol 5:49–59

Leone FA, Masui DC, Bezerra TMS, Garçon DP, Valenti VC, Augusto AS, McNamara JC (2012) Kinetic analysis of gill ($Na^+K^+$)-ATPase activity in selected ontogenetic stages of the Amazon River shrimp *Macrobrachium amazonicum* (Decapoda Palaemonidae): interactions at ATP- and cation-binding sites. J Membr Biol 245:201–215

Levenson R (1994) Isoforms of the NaK-ATPase: family members in search of function. Rev Physiol Biochem Pharmacol 123:1–45

Lima AG, McNamara JC, Terra WR (1997) Regulation of hemolymph osmolytes and gill ($Na^+$, $K^+$)-ATPase activities during acclimation to saline media in the freshwater shrimp Macrobrachium olfersi (Wiegmann 1836) (Decapoda Palaemonidae). J Exp Mar Biol Ecol 215:81–91

Lingrel JB (2010) The physiological significance of the cardiotonic steroid/ouabain-binding site of the NaK-ATPase. Annu Rev Physiol 72:395–412

Lopez LB, Quintas LEM, Noel F (2002) Influence of development on $Na^+/K^+$-ATPase expression: isoform- and tissue-dependency. Comp Biochem Physiol A 131:323–333

Lovett DL, Towle DW, Faris JE (1994) Salinity sensitive alkaline phosphatase activity in gills of the blue crab *Callinectes sapidus* (Rathbun). Comp Biochem Physiol B 109:163–173

Lucena MN, Garçon DP, Mantelatto FLM, Pinto MR, McNamara JC, Leone FA (2012) Hemolymph ion regulation and kinetic characteristics of the gill ($Na^+K^+$)-ATPase in the hermit crab *Clibanarius vittatus* (Decapoda Anomura) acclimated to high salinity. Comp Biochem Physiol B 161:380–391

Lucu C, Flik G (1999) $Na^+K^+$-ATPase and $Na^+/Ca^{2+}$ exchange activities in gills of hyperregulating *Carcinus maenas*. Am J Physiol Regul Integr Physiol 45:R490–R499

Lucu C, Towle DW (2003) ($Na^+K^+$)-ATPase in gills of aquatic crustacea. Comp Biochem Physiol A 135:195–214

Lucu C, Devescovi M, Siebers D (1989) Do amiloride and ouabain affect ammonia fluxes in perfused *Carcinus* gill epithelia. J Exp Zool 249:1–5

Mangum CP, Towle D (1977) Physiological adaptation to unstable environments. Am Sci 65:67–75

Martin DW, Sachs JR (2000) Ligands presumed to label high affinity and low affinity ATP binding sites do not interact in an $\alpha\beta_2$ diprotomer in duck nasal gland $Na^+K^+$-ATPase nor do the sites coexist in native enzyme. J Biol Chem 275:24512–24517

Masui DC, Furriel RPM, McNamara JC, Mantelatto FLM, Leone FA (2002) Modulation by ammonium ions of gill microsomal $Na^+K^+$-ATPase in the swimming crab *Callinectes danae*: a possible mechanism for regulation of ammonia excretion. Comp Biochem Physiol C 132:471–482

Masui DC, Furriel RPM, Silva EC, Mantelatto FLM, McNamara JC, Barrabin H, Scofano HM, Fontes CFL, Leone FA (2005) Gill microsomal ($Na^+K^+$)-ATPase from the blue crab *Callinectes danae*: interactions at cationic sites. Int J Biochem Cell Biol 37:2521–2535

Masui DC, Mantelatto FLM, McNamara JC, Furriel RPM, Leone FA (2009) $Na^+$, $K^+$-ATPase activity in gill microsomes from the blue crab Callinectes danae acclimated to low salinity: novel perspectives on ammonia excretion. Comp Biochem Physiol A 153:141–148

McNamara JC, Faria SC (2012) Evolution of osmoregulatory patterns and gill ion transport mechanisms in the decapod Crustacea: a review. J Comp Physiol B 182:997–1014

McNamara JC, Lima AG (1997) The route of ion water movements across the gill epithelium of the freshwater shrimp *Macrobrachium olfersii* (Decapoda, Palaemonidae): evidence from ultrastructural changes induced by acclimation to saline media. Biol Bull 192:321–331

McNamara JC, Moreira GS (1987) Oxygen consumption and acute salinity exposure in the freshwater shrimp *Macrobrachium olfersi* (Wiegmann) (Crustacea: Decapoda): whole animal and tissue respiration. J Exp Mar Biol Ecol 113:221–230

McNamara JC, Torres AH (1999) Ultracytochemical location of $Na^+$/$K^+$-ATPase activity and effects of high salinity acclimation in gill and renal epithelia of the freshwater shrimp *Macrobrachium olfersii* (Crustacea, Decapoda). J Exp Zool 284:617–628

Moretti R, Martin M, Proverbio T, Proverbio F, Marin R (1991) Ouabain-insensitive Na-ATPase activity in homogenates from different animal tissues. Comp Biochem Physiol 98:623–626

Morris MA, Greenaway P (1992) High affinity, $Ca^{2+}$ specific ATPase and ($Na^+$, $K^+$)-ATPase in the gill of the a supralittoral crab *Leptograpsus variegatus*. Comp Biochem Physiol 102A:15–18

Morth JP, Pedersen BP, Toustrup-Jensen MS, Sorensen TLM, Petersen J, Andersen JP, Vilsen B, Nissen P (2007) Crystal structure of the sodium-potassium pump. Nature 450:1043–1050

Neufeld GJ, Holliday CW, Pritchard JB (1980) Salinity adaption of gill NaK-ATPase in the blue crab *Callinectes sapidus*. J Exp Zool 211:215–224

New MB (1995) Status of freshwater prawn farming: a review. Aquac Res 26:1–54

Ogawa H, Shinoda T, Cornelius F, Toyoshima C (2009) Crystal structure of the sodium-potassium pump ($Na^+K^+$-ATPase) with bound potassium and ouabain. Proc Natl Acad Sci USA 106:13742–13747

Pedemonte CH, Beaugé LA (1983) Inhibition of ($Na^+K^+$)-ATPase by magnesium ions and inorganic phosphate and release of these ligands in the cycles of ATP hydrolysis. Biochim Biophys Acta 748:245–253

Pedersen PL, Amzel LM (1993) ATP synthases: structure reaction center mechanism in the regulation of one of nature's most unique machines. J Biol Chem 268:9937–9940

Péqueux A (1995) Osmotic regulation in crustaceans. J Crust Biol 15:1–60

Poulsen H, Morth P, Egebjerg J, Nissen P (2010) Phosphorylation of the $Na^+K^+$-ATPase e the $H^+K^+$-ATPase. FEBS Lett 584:2589–2595

Proverbio F, Marin R, Proverbio T (1991) The ouabain-insensitive sodium pump. Comp Biochem Physiol A 99:279–283

Read SM, Northcote DH (1981) Minimization of variation in the response to different proteins of the Coomassie blue-G dye–binding assay for protein. Anal Biochem 116:53–64

Reddy MS, Rao KV (1990) Aldrin and lindane impact on acid and alkaline phosphatase activities of prawn *Metapenaeus monoceros*: in vitro study. Biochem Int 22:1033–1040

Robinson JD (1970) Interactions between monovalent cations and the ($Na^+K^+$)-dependent adenosine triphosphatase. Arch Biochem Biophys 139:17–27

Robinson JD (1982) Tryptic digestion of the (NaK)-ATPase is both sensitive to and modifies $K^+$ interactions with the enzyme. J Bioenerg Biomembr 14:319–333

Santos LCF, Belli NM, Augusto A, Masui DC, Leone FA, McNamara JC, Furriel RPM (2007) Gill ($Na^+K^+$)-ATPase in diadromous freshwater palaemonid shrimps: species specific kinetic characteristics and α-subunit expression. Comp Biochem Physiol A 148:178–188

Segall L, Daly SE, Blostein R (2001) Mechanistic basis for kinetic differences between the rat α1, α2, and α3 isoforms of the ($Na^+$, $K^+$)-ATPase. J Biol Chem 276:31535–31541

Shinoda T, Ogawa H, Cornelius F, Toyoshima C (2009) Crystal structure of the sodium–potassium pump at 24 resolution. Nature 459:446–451

Silva ECC, Masui DC, Furriel RP, McNamara JC, Barrabin H, Scofano HM, Perales J, Teixeira-Ferreira A, Leone FA, Fontes CFL (2012) Identification of a crab gill FXYD2 protein and regulation of crab microsomal Na K-ATPase activity by mammalian FXYD2 peptide. Biochim Biophys Acta 1818: 2588–2597

Specht SC, Rodriguez C, Quinones L, Velazquez S (1997) Effect of high ionic strength and inhibitors of H K-ATPase on the ouabain sensitive K-*p*-nitrophenyl phosphatase activity in the sea anemone *Stichodactyla helianthus*. Comp Biochem Physiol B 117:217–224

Stern S, Borut A, Cohen D (1984) Characterization of ($Na^+$, $K^+$)-ATPase from the gills of the freshwater prawn Macrobrachium rosenbergii (De Man). Comp Biochem Physiol B 79:47–50

Sweadner KJ (1989) Isoenzymes of the $Na^+/K^+$-ATPase. Biochim Biophys Acta 988:185–220

Sweeney G, Klip A (1998) Regulation of the ($Na^+K^+$)-ATPase by insulin: why and how? Mol Cell Biochem 182:121–133

Takeyasu K, Tamkun M, Renaud KJ, Fambrough DM (1988) Ouabain-sensitive ($Na^+$-$K^+$)-ATPase activity expressed in mouse L cells by transfection with DNA encoding the α-subunit of an avian sodium pump. J Biol Chem 263:4347–4354

Taniguchi K, Kaya S, Abe K, Mardh S (2001) The oligomeric nature of Na/K-transport ATPase. J Biochem 129:335–342

Therien AG, Nestor NB, Ball NJ, Blostein R (1996) Tissue-specific versus isoform specific differences in cation activation kinetics of the NaK-ATPase. J Biol Chem 271:7104–7112

Torres G, Charmantier-Daures M, Chifflet S, Anger K (2007) Effects of long-term exposure to different salinities on the location and activity of $Na^+$-$K^+$-ATPase in the gills of juvenile mitten crab *Eriocheir sinensis*. Comp Biochem Physiol 147:460–465

Towbin H, Staehelin T, Gordon J (1979) Electrophoretic transfer of proteins from polyacrylamide gels to nitrocellulose sheets—procedure and some applications. Proc Nat Acad Sci USA 76:4350–4354

Towle DW (1997) Molecular approaches to understanding salinity adaptation of estuarine animals. Am Zool 37:575–584

Towle DW, Holleland T (1987) Ammonium ion substitutes for $K^+$ in ATP-dependent $Na^+$ transport by basolateral membrane vesicles. Am J Physiol Regul Integr Physiol 252:R427–R489

Towle DW, Taylor DD (1976) Effect of $NH_4^+$ and $K^+$ on $Na^+$-transport ATPase activity of blue-crab gill. Am Zool 16:224

Towle DW, Weihrauch D (2001) Osmoregulation by gills of euryhaline crabs: molecular analysis of transporters. Am Zool 41:770–780

Toyoshima C, Kanai R, Cornelius F (2011) First crystal structures of $Na^+K^+$-ATPase: new light on the oldest ion pump. Structure 19:1732–1738

Tribuzy AVB, Fontes CFL, Norby JG, Barrabin H (2002) Dimethylsulfoxide-induced conformational state of $Na^+/K^+$-ATPase studied by proteolytic cleavage. Arch Biochem Biophys 399:89–95

Wall SM (1996) Ammonium transport and the role of the NaK-ATPase. Miner Electrol Metab 22:311–317

Ward DG, Cavieres JD (1998) Photoinactivation of fluorescein isothiocyanate-modified NaK-ATPase by 2′(3′)-*O*-(2,4,6-trinitrophenyl) 8-azidoadenosine 5′-diphosphate—abolition of E1 and E2 partial reactions by sequential block of high and low affinity nucleotide sites. J Biol Chem 273:14277–14284

Weihrauch D, Becker W, Postel U, Riestenpatt S, Siebers D (1998) Active excretion of ammonia across the gills of the shore crab *Carcinus maenas* and its relation to osmoregulatory ion uptake. J Comp Physiol B 168:364–376

Weihrauch D, Becker W, Postel U, Luck-Kopp S, Siebers D (1999) Potential of active excretion of ammonia in three different haline species of crabs. J Comp Physiol B 169:364–376

Weihrauch D, McNamara JC, Towle DW, Onken H (2004) Ion-motive ATPases and active transbranchial NaCl uptake in the red freshwater crab *Dilocarcinus pagei* (Decapoda Trichodactylidae). J Exp Zool 207:4623–4631

Wilder MN, Ikuta K, Atmomarsono M, Hatta T, Komuro K (1998) Changes in osmotic and ionic concentrations in the hemolymph of *Macrobrachium rosenbergii* exposed to varying salinities and correlation to ionic and crystalline composition of the cuticle. Comp Biochem Physiol A 119:941–950

Wilder MN, Huong DTT, Atmomarsono M, Hien TTT, Phu TQ, Yang WJ (2000) Characterization of Na/K-ATPase in *Macrobrachium rosenbergii* and the effects of changing salinity on enzymatic activity. Comp Biochem Physiol A 125:377–388